CARDIFF UNIVERSITY
PRIFYSGOL CAERDYDD

# ORCA – Online Research @ Cardiff

This is an Open Access document downloaded from ORCA, Cardiff University's institutional repository:https://orca.cardiff.ac.uk/id/eprint/70605/

This is the author's version of a work that was submitted to / accepted for publication.

Citation for final published version:

Ingavle, Ganesh C., Baillie, Les , Zheng, Yishan, Lis, Elzbieta K., Savina, Irina N., Howell, Carol A., Mikhalovsky, Sergey V. and Sandeman, Susan R. 2015. Affinity binding of antibodies to supermacroporous cryogel adsorbents with immobilized protein A for removal of anthrax toxin protective antigen. Biomaterials 50 , pp. 140-153. 10.1016/j.biomaterials.2015.01.039

Publishers page: http://dx.doi.org/10.1016/j.biomaterials.2015.01.0...

Please note:
Changes made as a result of publishing processes such as copy-editing, formatting and page numbers may not be reflected in this version. For the definitive version of this publication, please refer to the published source. You are advised to consult the publisher's version if you wish to cite this paper.

This version is being made available in accordance with publisher policies. See http://orca.cf.ac.uk/policies.html for usage policies. Copyright and moral rights for publications made available in ORCA are retained by the copyright holders.

Biomaterials 50 (2015) 140–153

Contents lists available at ScienceDirect

Biomaterials

journal homepage: www.elsevier.com/locate/biomaterials

# Affinity binding of antibodies to supermacroporous cryogel adsorbents with immobilized protein A for removal of anthrax toxin protective antigen

Ganesh C. Ingavle [a, 1], Les W.J. Baillie [b, 2], Yishan Zheng [a, 1], Elzbieta K. Lis [b, 2], Irina N. Savina [a, 1], Carol A. Howell [a, 1], Sergey V. Mikhalovsky [a, c, 1], Susan R. Sandeman [a, *]

[a] Biomaterials and Medical Devices Research Group, School of Pharmacy and Biomolecular Sciences, Huxley Building, University of Brighton, Brighton, East Sussex BN2 4GJ, UK
[b] School of Pharmacy and Pharmaceutical Sciences, Cardiff University, Redwood Building, King Edward VII Avenue, Cardiff CF10 3NB, UK
[c] School of Engineering, Nazarbayev University, 53 Kabanbay Batyr Ave., Astana 010000, Kazakhstan

ARTICLE INFO

*Article history:*
Received 30 September 2014
Accepted 20 January 2015
Available online

*Keywords:*
Supermacroporous cryogel
Anthrax toxin protective antigen (PA)
Protein A affinity cryogels
Anthrax toxin specific monoclonal antibodies

ABSTRACT

Polymeric cryogels are efficient carriers for the immobilization of biomolecules because of their unique macroporous structure, permeability, mechanical stability and different surface chemical functionalities. The aim of the study was to demonstrate the potential use of macroporous monolithic cryogels for biotoxin removal using anthrax toxin protective antigen (PA), the central cell-binding component of the anthrax exotoxins, and covalent immobilization of monoclonal antibodies. The affinity ligand (protein A) was chemically coupled to the reactive hydroxyl and epoxy-derivatized monolithic cryogels and the binding efficiencies of protein A, monoclonal antibodies to the cryogel column were determined. Our results show differences in the binding capacity of protein A as well as monoclonal antibodies to the cryogel adsorbents caused by ligand concentrations, physical properties and morphology of surface matrices. The cytotoxicity potential of the cryogels was determined by an *in vitro* viability assay using V79 lung fibroblast as a model cell and the results reveal that the cryogels are non-cytotoxic. Finally, the adsorptive capacities of PA from phosphate buffered saline (PBS) were evaluated towards a non-glycosylated, plant-derived human monoclonal antibody (PANG) and a glycosylated human monoclonal antibody (Valortim®), both of which were covalently attached via protein A immobilization. Optimal binding capacities of 108 and 117 mg/g of antibody to the adsorbent were observed for PANG attached poly(acrylamide-allyl glycidyl ether) [poly(AAm-AGE)] and Valortim® attached poly(AAm-AGE) cryogels, respectively, This indicated that glycosylation status of Valortim® antibody could significantly increase (8%) its binding capacity relative to the PANG antibody on poly(AAm-AGE)-protien-A column ($p < 0.05$). The amounts of PA which remained in the solution after passing PA spiked PBS through PANG or Valortim bound poly(AAm-AGE) cryogel were significantly ($p < 0.05$) decreased relative to the amount of PA remained in the solution after passing through unmodified as well as protein A modified poly(AAm-AGE) cryogel columns, indicates efficient PA removal from spiked PBS over 60 min of circulation. The high adsorption capacity towards anthrax toxin PA of the cryogel adsorbents indicated potential application of these materials for treatment of *Bacillus anthracis* infection.

© 2015 The Authors. Published by Elsevier Ltd. This is an open access article under the CC BY-NC-ND license (http://creativecommons.org/licenses/by-nc-nd/4.0/).

## 1. Introduction

Anthrax toxin is produced by *Bacillus anthracis*, the causative agent of anthrax, and is responsible for the major symptoms of the disease [1]. The toxin consists of a single receptor-binding moiety, termed protective antigen (PA), and two enzymatic moieties, termed edema factor (EF) and lethal factor (LF) [2]. After release from the bacteria as nontoxic monomers, these three proteins

* Corresponding author. Tel.: +44 01273 641377.
*E-mail addresses:* g.c.ingavle@brighton.ac.uk (G.C. Ingavle), BaillieL@cardiff.ac.uk (L.W.J. Baillie), yz9@brighton.ac.uk (Y. Zheng), LisE@cardiff.ac.uk (E.K. Lis), I.N.Savina@brighton.ac.uk (I.N. Savina), C.A.Howell@brighton.ac.uk (C.A. Howell), S.Mikhalovsky@brighton.ac.uk (S.V. Mikhalovsky), s.sandeman@brighton.ac.uk (S.R. Sandeman).
[1] Tel.: +44 01273 641912.
[2] Tel.: +44 (0)29 208 75535.

http://dx.doi.org/10.1016/j.biomaterials.2015.01.039
0142-9612/© 2015 The Authors. Published by Elsevier Ltd. This is an open access article under the CC BY-NC-ND license (http://creativecommons.org/licenses/by-nc-nd/4.0/).

diffuse to the surface of a mammalian cell and assemble into toxic, cell–bound complexes. Although a vaccine against anthrax exists, various aspects make mass vaccination unfeasible. In the event of a bioterrorist attack, antibiotic treatment of inhalational anthrax victims is effective if started shortly after exposure but may be less effective if delayed even by few hours [3]. Guidelines from the US Centers for Disease Control and Prevention recommend that individuals who have inhaled spores should receive at least 60 days of antibiotic treatment as well as a post exposure vaccination [4]. An alternative approach to vaccination is the administration of preformed toxin neutralising antibodies which have the capacity to confer instant immunity. A number of therapeutic human monoclonal antibodies have been developed such as Raxibacumab [5] or are in process of being developed such as Valortim® and a non-glycosylated, plant-produced human monoclonal antibody (PANG) [6].

Valortim® is a fully human anti-toxin monoclonal antibody which is being developed for the prevention and treatment of inhalational anthrax. It neutralizes lethal toxin cytotoxicity by binding to the carboxy-terminal region of PA [7]. Preclinical studies suggest that Valortim® has the potential to provide protection against anthrax infection when administered prophylactically (prior to the emergence of symptoms of anthrax infection) and also may increase survival when administered therapeutically [7,8]. PANG is also being developed as a post exposure therapy for the treatment of *B. anthracis* [6]. Like Valortim® it has been shown to be effective in primate studies and recognises the carboxy-terminal region of PA although the precise site has yet to be determined. Unlike Valortim® this human derived antibody is produced from plants and consequently has been de-glycosylated to increase its *in vivo* half-life. While experiments to date have focused on delivering these antibodies by injection there is interest in assessing their efficacy as part of a hemoperfusion system. An effective route of administration has yet to be demonstrated.

Macroporous monolithic materials produced from hydrophilic monomers and polymers by cryogelation techniques have previously been used for biomedical applications [9–13] [Fig.1]. Cryogelation is a process of gel formation, which takes place in a semi-frozen state [14]. The cryogelation technique allows preparation of elastic, mechanically stable monolithic matrices with large interconnected pores easily permeable to aqueous solutions of proteins and suspensions of cells. The monolithic gels exhibit multiple interconnected pores of 1–100 μm in diameter [15]. The pore size can be controlled by changing the synthesis parameters including the nature of monomer and polymer type, temperature and cross-linker composition. An attractive feature of the cryogelation technique is the possibility of macropore formation in which large interconnected pores ensure a large surface area for bioligand attachment allowing the production of adsorptive materials with a high capacity towards a target compound. This has recently been demonstrated by the use of a polystyrene microparticle embedded composite cryogel to effectively adsorb liver toxins such as bilirubin, bile acid, and aromatic amino acids indicating a potential application for extracorporeal blood purification for the removal of liver toxins [16].

Introduction of epoxy and hydroxyl functionality into cryogel composition is a common approach for the preparation of cryogels for further functionalization with bioactive reagents. For example, the epoxy group of glycidyl methacrylate (GMA) is hydrolysed to create an aldehyde groups which can be easily coupled to an amine-containing ligand. Zou et al. used this approach to immobilize protein A onto modified poly(glycidyl methacrylate-co-trimethylolpropane trimethacrylate) and poly(glycidyl methacrylate-co-ethylene glycol dimethacrylate) monoliths for affinity chromatography [17]. The column was used for analysis of human immunoglobulin G (hIgG).

Fundamental issues in the improvement of the antibody–antigen interaction are optimised antibody immobilisation and antigen capture efficiency [18,19]. Immobilized antibodies on a porous polymer surface utilise the binding specificity of antibody–antigen pairing to remove biotoxin. However antigen adsorption relies on the bioactivity and binding efficiency of the pre-immobilised antibody, requiring careful optimisation of the bioligand binding strategy. The optimum immobilization requirement is usually met by ensuring a high density of active antibodies on the polymer surface [20]. Immobilization of antibodies simply by physical adsorption might have problems in stability [21–24] and hence a covalent binding method for immobilization is preferred [25–27]. This is accomplished by derivatizing the surfaces with suitable functional groups with covalent attachment of antibodies. Antibodies have been immobilised onto the surface of various substrates like glass, gold, plastics, membranes, and gel pads [28,29].

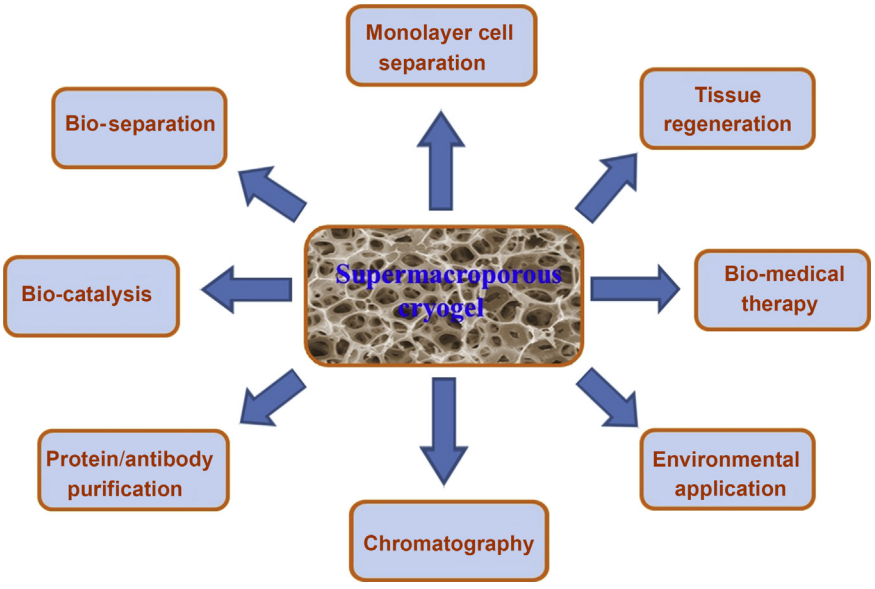


**Fig. 1.** Schematic diagram showing diverse applications of supermacroporous cryogels.

Several methods have been used for immobilizing monoclonal antibodies on solid supports [30]. Binding properties of immunosorbents are strongly influenced by the load, surface density and orientation of the immobilized antibodies [31]. The antibody should be attached in a way that preserves the antibody active sites for interaction with antigen. Because of this, the density of immobilized antibodies on the support and antibody activity have to be controlled and both multiple-site attachment and random orientations must be avoided [32]. One of the methods used to orient IgG molecules on solid surfaces is binding of the antibody to a protein A-activated support and then crosslinking of the antibody to protein A through covalent linkage [33,34]. Oriented coupling techniques, such as those using protein A, increase both the antigen-binding capacity [35–37] and the efficiency of the immunosurfaces [38]. For improved orientation of the immobilized antibody molecules, one of the most common methods employed is the immobilization of antibodies at the Fc region through the use of protein A [36,37]. The functionally oriented immobilized antibodies are produced by binding of the constant heavy chain region (Fc) of the IgG molecule to protein A, which leaves the variable heavy and light chain regions (Fab) available for binding to antigen epitopes [34].

There is no detailed study of covalently immobilized antibody adsorption of anthrax toxin PA on macroporous cryogel columns with different mechanical and physical properties. In this paper, we report for the first time the covalent immobilization of *B. anthracis* exotoxin specific antibodies PANG and Valortim® on crosslinked macroporous polymer columns having epoxy and hydroxyl functionalities, synthesized by a cryogelation method, for the removal of anthrax protective antigen from PBS. For maximum PA adsorption on antibody bound cryogel columns, all the individual cryogel materials, have been separately optimized in terms of polymer composition, crosslinker type, protein A attachment, mechanical as well as physical properties of cryogel support and flow rate. The adsorption of anthrax toxin protective antigen (PA) was assessed on antibody bound monolithic cryogels with immobilized protein A. The affinity ligand (protein A) was chemically coupled to the reactive epoxy and hydroxyl-derivatized monolithic cryogels through different immobilization techniques and the binding efficiency of the protein A and antibody towards cryogel columns was determined. Although both antibodies targeted PA they differed in their physical properties, one was human derived and the other was produced by a plant and was subsequently de-glycosylated, thus we sort to determine if these differences influenced their ability to bind to protein A and subsequently capture PA.

## 2. Materials and method

### 2.1. Materials

The basic monomers and reagents, acrylamide (AAm, 99%), 2-hydroxyethylmethacrylate (HEMA), poly(ethylene glycol) diacrylate (PEGDA) (average Mn ~258), N′, N′-methylene-bis(acrylamide) (MBA, 99%), allyl glycidyl ether (AGE, 99%), glutaraldehyde, ethanolamine, bicinchoninic acid protein reagent, Cu(II) sulfate solution, N, N, N′, N′-tetra-methyl-ethylenediamine (TEMED), Dimethyl pimelimidate (DMP), and protein A from *Staphylococcus aureus* were obtained from Sigma (St Louis, MO, USA). Ammonium persulfate (APS, 98%), and ethylenediamine (EDA, 99%) were purchased from Aldrich (Steinheim, Germany). Poly(vinyl alcohol) (PVA), Mowiol 18–88, Mw = 130000 g $mol^{-1}$, saponification degree of 88%, was purchased from Clariant GmbH (Frankfurt, Germany). Triethanolamine and sodium borohydride ($NaBH_4$) were obtained from Merck (Darmstadt, Germany). PANG antibody was obtained from Fraunhofer USA Inc, (Delaware, USA), while Valortim® antibody was kindly donated by PharmAthene Inc. (Maryland, USA). The PA gene was cloned into a pQE30 vector (with a His-tag added), expressed in *E. coli* and purified as described by Stokes et al. [39].

### 2.2. PVA-GA cryogel preparation

The PVA cryogels were synthesized by a cryogelation technique (Fig. 2) based on the method developed by Plieva et al. [40]. A stock of 10% (w/v) PVA solution was prepared by dissolving 10 g of PVA in 100 mL distilled water at 90°C in a heated water bath whilst stirring. Once the PVA was completely dissolved, the solution was cooled to room temperature with constant stirring. The PVA stock solution was stored at room temperature. To prepare the PVA cryogels, the stock PVA solution was diluted to achieve a 5% w/v PVA concentration and adjusted to pH 1.0–1.2 by adding 5 M hydrochloric acid drop wise. Chilled 25% (w/v) glutaraldehyde solution in water was added to the pH adjusted and chilled PVA solution to give a final concentration of 1% and 2% (w/v). The solution was stirred for 30 s and then 0.5 mL or 1.0 mL solution pipetted in 7 mm or 9 mm inner diameter glass tube moulds closed at the bottom with a silicon cap and placed in a −12°C ethanol bath for 18 h. The PVA cryogel columns were defrosted at room temperature and washed with water until the pH stabilised at 6.5. The resulting cryogel samples were named PVA cryogels.

### 2.3. Preparation of AAm-AGE cryogel

Epoxy-containing supermacroporous monolithic poly(AAm-AGE) cryogels were produced by dissolving the monomers (0.954 g AAm, 0.266 g of MBA and 0.358 mL of AGE in deionized water (final concentration 8%). Free radical polymerization was initiated by adding TEMED (20 μL) and APS (20 mg). The reaction mixture was poured into glass tubes (8 × 11 mm i.d.) and was frozen at −12°C for 18 h. The cryogel was thawed at room temperature and after washing with water the cryogel columns were stored at 4°C. The resulting cryogel samples were named AAm-AGE cryogels.

### 2.4. Preparation of poly(HEMA-co-MBA) and poly(HEMA-co-PEGDA) cryogels

Monomers (0.8 mL HEMA and 0.2 g N, N′-methylene-bis(acrylamide) (MBA) were dissolved in deionized (DI) water (10 mL) and the mixture was degassed under vacuum for 5 min to eliminate soluble oxygen. Total concentration of monomers was 8% (w/v). The cryogel was produced by free radical polymerization initiated by TEMED and APS. After adding TEMED (20 μL, 1% (w/v) of the total monomers) the solution was cooled in an ice bath for 15 min. APS (20 mg, 1% (w/v) of the total monomers) was added and the reaction mixture was stirred for 30 s and then 1.0 mL solution pipetted in 9 mm inner diameter glass tube moulds closed at the bottom with a silicon cap. The polymerization solutions in the glass tubes were frozen at −12°C for 18 h and then thawed at room temperature. After washing with 200 mL of water, the cryogel was stored at 2–8°C until further used. Poly(HEMA-co-PEGDA) cryogel was synthesized according to the protocol described above. The co-monomers were mixed at a ratio of 1:2 (PEGDA: HEMA) (final concentration 8% v/v). The resulting cryogel samples were named HEMA-PEGDA cryogels.

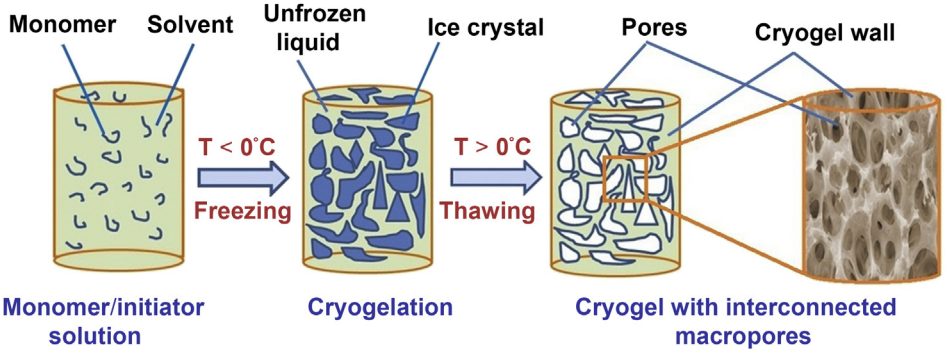


**Fig. 2.** Different stages during formation of cryogel having interconnected macropores.

### 2.5. Protein A attachment on cryogel surface via epoxy and hydroxyl functional groups

#### 2.5.1. On epoxy containing cryogels

The epoxy-containing porous monolithic AAm-AGE cryogel was first treated with ethylenediamine, then glutaraldehyde (GA) and then protein A was attached through an aldehyde group (Fig. 3A). The 1 mL cryogel columns (length = 1.5 cm, i.d = 9 mm, number of columns, n = 3) were connected to a peristaltic pump and washed simultaneously with 20 mL of water, at a flow rate of 1 mL/min and then with 0.2 M $Na_2CO_3$ (20 mL). Ethylenediamine (0.5 M in 0.2 M $Na_2CO_3$; 30 mL) was applied to the columns at a flow rate of 1 mL/min in recycle mode for 4 h. After washing with water until the pH was close to neutral, the column was washed with 20 mL 0.1 M sodium phosphate buffer, pH 7.2. A solution of glutaraldehyde (5% v/v; 30 mL) in 0.1 M sodium phosphate buffer, pH 7.2, was applied to the column at a flow rate of 1 mL/min in recycle mode for 5 h. The derivatized matrix with functional aldehyde groups was used for coupling of protein A. The solution of protein A (2 mg/mL; 12 mL) in 0.1 M sodium phosphate buffer, pH 7.2, was recycled through each column at a flow rate of 1 mL/min at 4°C for 24 h. Finally, the freshly prepared $NaBH_4$ solution (0.1 M in sodium carbonate buffer, pH 9.2; 30 mL) was applied to the column at a flow rate of 1 mL/min for 3 h in recycle mode to reduce Schiff's base formed between the protein and the aldehyde containing matrix.

#### 2.5.2. On hydroxyl containing cryogels

The hydroxyl groups presented on the PVA, HEMA-MBA, and HEMA-PEGDA cryogel 1 mL columns (length = 1.5 cm, i.d = 9 mm, n = 3) were activated with cyanogen bromide (CNBr) in order to prepare active attachment sites for protein A (Fig. 3B). Prior to the activation process, cryogels (n = 3) were kept in distilled water for about 24 h and washed with 0.5 M NaCl solution and water. 2 mL of 0.5 M sodium carbonate buffer (pH 10.5) was added and the solution was stirred slowly. The mixture was placed in a fume hood and the glass pH electrode was immersed into this solution. The CNBr (1 mL, 0.5 M) solution was prepared and added to the mixture. The pH of this solution was quickly adjusted to 11.5 with 4M NaOH and the pH was maintained between 10.5 and 11.5 during the activation reaction. The CNBr solution was recirculated through the column at 1 mL/min at room temperature and activation procedure was continued for 50–60 min. Cryogels were washed thoroughly with 0.1 M $NaHCO_3$ in order to remove residual or unreacted activation agent. Then, the CNBr-activated cryogel columns were washed 3–4 times with distilled water containing 0.5 M NaCl. The washed cryogel columns were treated with 50 mL of carbonate buffer (pH 10) at 1 mL/min for 1 h. Then, 50 mL of protein A solution (2.0 mg/mL, pH 6.5) was pumped through the column under recirculation at 1.0 mL/min for 2 h. Finally, non-covalently adsorbed protein A was removed by washing the cryogel column with borate buffer.

### 2.6. PANG and Valortim® antibody binding

PANG and Valortim® antibodies were coupled to the protein A modified PVA, AAm-AGE, HEMA-MBA, and HEMA-PEGDA cryogel columns as follows (Fig. 4). The protein–cryogel columns were washed with 50 mM sodium borate, pH 8.2. PANG or Valortim® antibody (1 mL; 2 mg/mL) in 50 mM sodium borate, pH 8.2 was recirculated through the cryogel columns at 1.0 mL/min for 1 h. Columns were washed thoroughly with 50 mM sodium borate, pH 8.2 and 0.2 M triethanolamine, pH 8.2. A solution of DMP (6.6 mg/mL, 5 mL) in 0.2 M triethanolamine, pH 8.2 was applied to the column at a flow rate of 1 mL/min in recycle mode for 1 h at room temperature. Columns were washed with water. Ethanolamine (0.1 M; 5 mL), pH 8.2, was recirculated through the columns for 10 min to block any remaining active sites. Finally, columns were washed with water, 1 M NaCl, and 0.1 M glycine to remove the non-covalently bound antibody from the protein sections.

### 2.7. Bioligand content determination

The amount of covalently attached protein A and antibody on monolithic cryogel matrix was determined by the bicinchoninic acid (BCA) method. An appropriate amount of dried protein or antibody coupled cryogel pieces were well suspended in water by finely grinding and ultrasonication. Two mL of the BCA solution was added to different amounts of the protein and antibody coupled cryogel column suspensions (20–100 μL) and the mixture was incubated at 37°C with thorough shaking for 30 min. The absorbance was measured at 562 nm both with and without centrifuging the samples. Appropriate controls were taken using native unmodified cryogel. The standard curve was made by using a known concentration of protein and IgG standard from 0, 200, 400, 600, 800, and 1000 μg/mL.

### 2.8. FTIR characterisation

In order to characterize the crosslinking polymers and protein A attachment, infrared measurements were carried out with Universal ATI, PerkinElmer (Spectrum

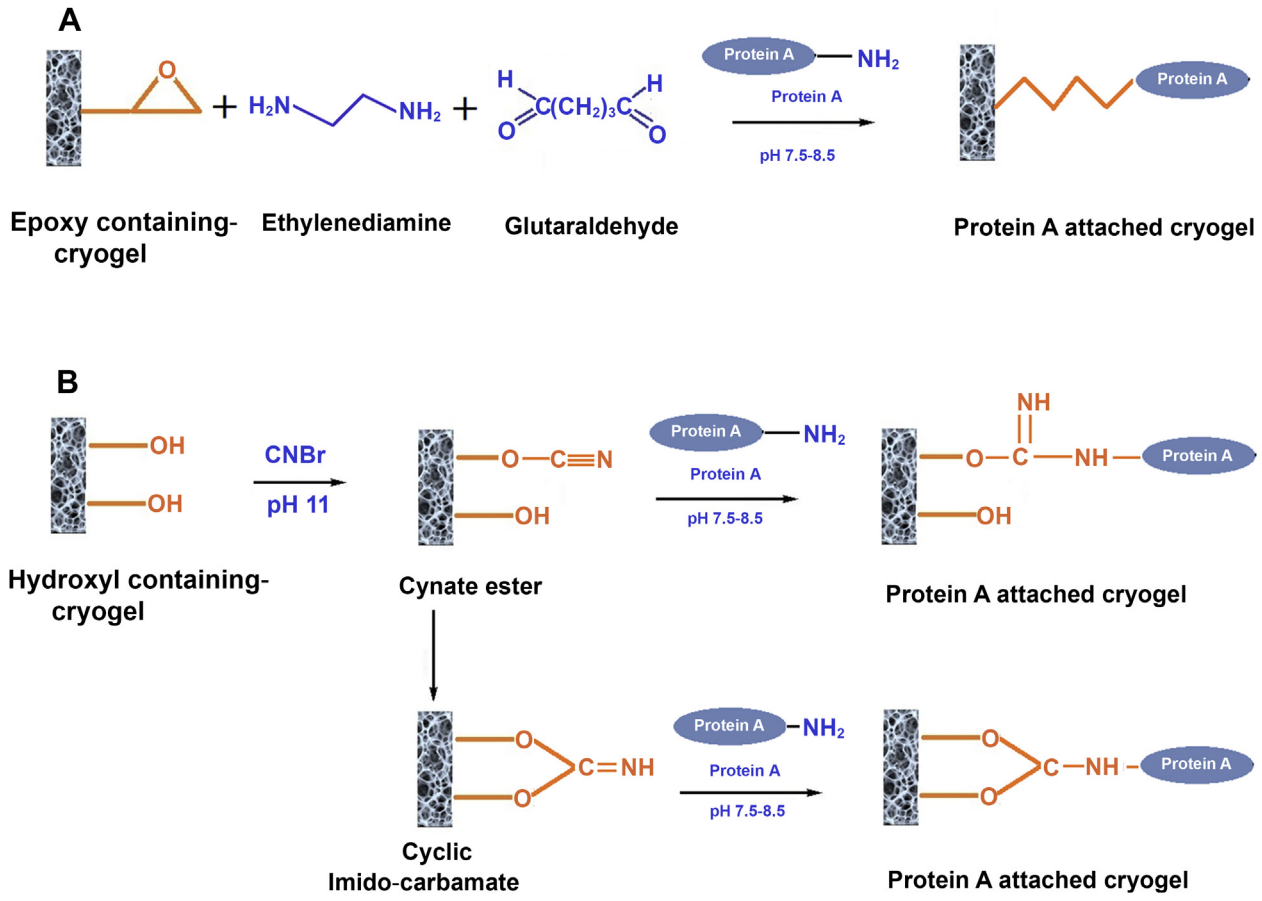


**Fig. 3.** Schematic representation illustrating different pathways to activate hydroxyl and epoxy containing cryogels for protein A attachment.

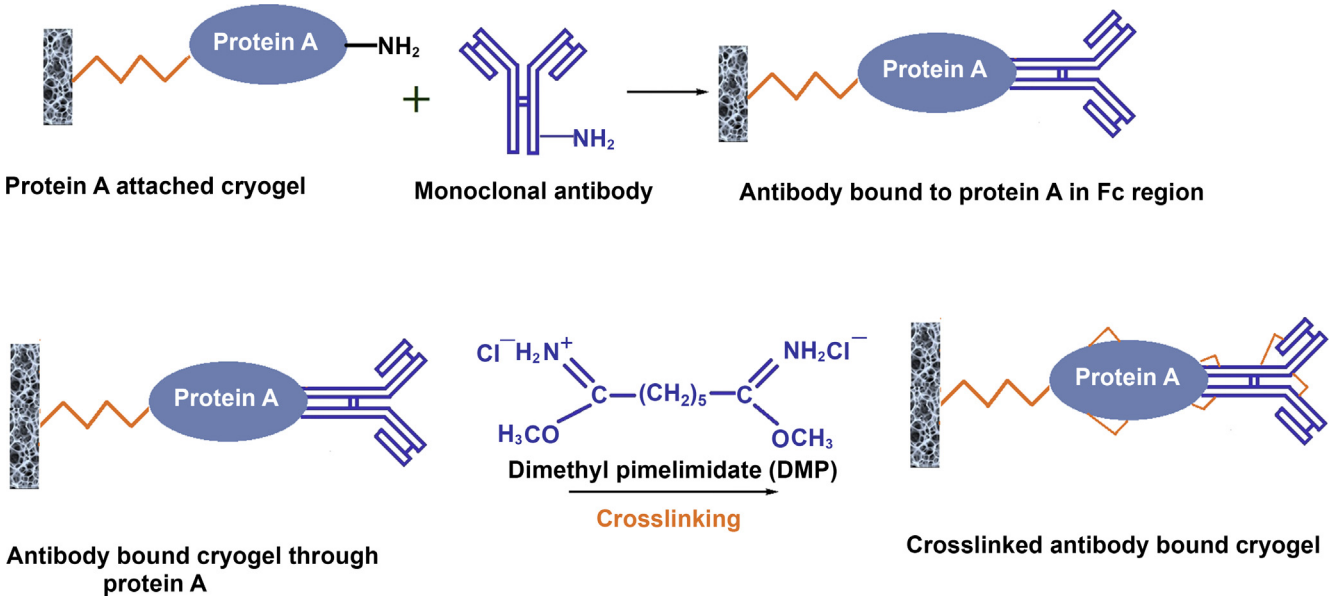


**Fig. 4.** Schematic representation illustrating covalent crosslinking between IgG and immobilized protein A via dimethyl pimelimidate (DMP).

650) FT-IR spectrometer, USA. FTIR spectra were obtained in the range of 4000–400 $cm^{-1}$ during 64 scans, with 2 $cm^{-1}$ resolution, using diffuse reflectance mode.

### 2.9. Scanning electron microscopy (SEM)

For SEM imaging, the fully hydrated 1 mL cryogel columns were sectioned to a thickness of 1 mm. To avoid ice formation altering the existing cryogel internal structure, prior to the freeze drying processes, low temperature instant freezing was employed to encourage the formation of smaller ice crystals. Therefore, sections of cryogel samples were frozen at −80°C before being transferred to a Christ freeze dryer to remove the water from the cryogel matrix over night at 0.200 mbar vacuum pressures. The freeze-dried cryogel slices were mounted on a sample holder and coated with a 4 nm thick layer of platinum using a Quorum (Q150TES) coater. The sections were examined using a Zeiss Sigma field emission gun SEM (Zeiss NTS) at an accelerating voltage of 5 kV at 100, 500, and 1000× magnifications.

### 2.10. Confocal microscopy

Confocal microscopy was used to allow the imaging of the porosity and internal structure of cryogels in a hydrated state. For confocal imaging, the fully hydrated 1 mL cryogels were sliced into 1 mm thick sections and transferred into a 24 well-plate containing 1 mL of 50 μM Rhodamine B. The cryogel slices were incubated with the Rhodamine B dye in the dark for 30 min before Rhodamine B solution was removed and the sample slices were washed with water until no pink colour was observed. The cryogel slices were kept hydrated during the confocal microscopy (Leica TCS SP5, Wetzlar, Germany). Images were obtained using an excitation wavelength of 562 nm and detected using an emission wavelength of 573 nm.

### 2.11. Swelling properties of cryogels

Cryogel 1 mL columns (n = 3) were placed in excess DI water for at least 24 h to remove extractable materials from polymer networks. Equilibrated cryogel columns samples were weighed and placed into an oven at 60°C. After at least 48 h, the dried gel samples were removed and weighed again. The equilibrium swelling degree, Q, was defined as the ratio of the fully swollen cryogel mass to that of its dry mass.

### 2.12. Mechanical testing

The compressive moduli of the cryogel columns were determined at room temperature on a TA.XT Plus Texture Analyser (from Stable Micro System) and tested under unconfined uniaxial compression with a 5N load cell. The cryogel dimensions were measured with calipers under a stereomicroscope. All measurements and mechanical testing were performed on cryogels swollen to equilibrium in DI water. Following a tare load of 5N, cryogels were then compressed in the direction normal to the circular face of the cryogel at a rate of 0.05 mm/s. The compressive elastic modulus, defined as the slope of the linear region of the stress–strain curve of a material under compression, was calculated from the initial linear portion of the curve (<20% strain). The moduli were reported as mean values from sets of at least 5 samples.

### 2.13. Specific surface area

For nitrogen adsorption analysis, the cryogels samples were frozen at −80°C for 30 min before being transferred to a Christ freeze dryer overnight under 0.200 mbar vacuum pressure for the removal of water present in the cryogel pores. The freeze dried cryogel samples used for low temperature nitrogen adsorption analysis were degassed for 24 h at 50°C using an Autosorb-1 gas sorption analyser (Quantachrome Instruments, USA). The relatively low temperature of 50°C was selected in order to preserve the cryogel polymeric structure. The instrument (Autosorb-1 gas sorption analyser, Quantachrome Instruments, USA) was used to measure the adsorbed and desorbed volumes of nitrogen by the test samples at relative pressures at 77.4 K. The data were analysed using Quantachrome data analysis software (Quantachrome ASiQwin). The specific surface area was calculated using the Brunauer, Emmett and Teller (BET) equation.

### 2.14. Cell viability and cytotoxicity assay

Fibroblast type hamster lung cell line V79 were chosen as they are a cell line considered to be sensitive to cytotoxic effects [41]. The V79 cells were maintained in 10% FBS supplemented DMEM medium with 1% penicillin/streptomycin and passaged by trypsinization at 80% confluence approximately every two days. To optimise the cell seeding density for the LDH and MTS assays, a series of cell seeding densities in 100 μl medium ($5.00 \times 10^4$, $2.50 \times 10^4$, $1.25 \times 10^4$, $0.63 \times 10^4$, $0.31 \times 10^4$, $0.16 \times 10^4$, and $0.08 \times 10^4$ cells/well) were added to each well of a 96 well plate and incubated for 24 h. The utilisation of MTS and the release of LDH by the cultured cells were determined using 5- (3 − carboxymethoxyphenyl) − 2(4, 5 − dimethylthiazoly) − 3 − (4-sulfophenyl) tetrazolium, inner salt (MTS) and lactic dehydrogenase (LDH) assay kits following the manufacturer's protocol (Promega, Corp., Madison, WI).

#### 2.14.1. Extract preparation and cell extract treatment

Material extracts were prepared by incubating 0.5 g of freeze dried cryogel in 3 mL of 10% fetal bovine serum (FBS) supplemented phenol-red free DMEM medium at 37°C for 24 h. A positive control of dibutyltin maleate containing PVC polymer and a negative control containing culture media only were also included. The extracts were sterilized by filtering through a 0.2 μm syringe filter before being used undiluted (100%). In addition, a 50% dilution of the sterilised extracts was also prepared for cell treatment by adding 50% of fresh culture. V79 cells were seeded into a 96-well-plate at a density of $1 \times 10^4$ cells per well and incubated at 37°C in a humidified 5% $CO_2$ atmosphere for approximately 18 h prior to extract treatment. The 18 h incubation period was selected to allow the cells to settle onto the culture plate but also to avoid prolonged incubation resulting in over populated culture conditions. Medium was removed and extracts were introduced in triplicates. The cells were incubated with extract samples for a further 8 or 24 h before the MTS and LDH assays were performed.

#### 2.14.2. MTS assay

After the extract incubation time, the culture medium was aspirated and 100 μL of 20% (v/v) MTS reagent in phenol red free medium was added to each well of the plate followed by further 2 h incubation at 37°C in a humidified 5% $CO_2$ atmosphere.

The MTS formazan intensity was measured at 492 nm using a Biotech ELISA plate reader. The cell viability was calculated according to Equation (1), where $I_0$ represents the intensity of MTS formazan produced by V79 cells exposed to the culture medium; $I_1$ represents the intensity of MTS formazan produced by V79 cells exposed to the sample extracts; B is the media blank.

$$\text{Viability\%} = (I_1 - B)/I_0 \times 100\% \quad (1)$$

#### 2.14.3. LDH assay

After the extract incubation period, 50 μL aliquots of culture medium were transferred to a fresh 96-well plate, and 50 μL of LDH substrate solution was added to react with the LDH released by the V79 cells in the culture medium. The plates were left in the dark at room temperature for 30 min before 50 μL of stop solution was added to each well of the plate. The intensity of LDH formazan product was measured at 492 nm using a Biotech ELISA plate reader. The cytotoxicity was calculated according to Equation (2), where $I_0$ represents the intensity of LDH formazan released by V79 cells when the cells were lysed; $I_1$ represents the intensity of LDH formazan released by V79 cells exposed to the sample extracts; B is the medium blank.

$$\text{Cytotoxicity \%} = (I_1 - B)/I_0 \times 100\% \quad (2)$$

### 2.15. Timed PA adsorption on antibody coupled cryogels

AAm-AGE columns having maximum binding capacities towards PANG and Valortim® antibodies were selected to assess PA adsorption. Phosphate buffered saline (PBS) was spiked with the anthrax toxin protective antigen (PA) at a concentration of 1 μg/mL. PBS was recirculated through PANG and Valortim® antibody bound AAm-AGE cryogel columns (n = 3, length = 1.5 cm, dia = 9 mm) having high protein A capacity at a flow rate of 1 mL/min for 1 h at room temperature prior to adsorption of PA. 1000 μL of PA spiked PBS was recirculated at a flow rate of 2 mL/min through each of the cryogel columns, controls consisted of PA spiked PBS, or PBS without PA. At 15, 30, 45 & 60 min time points, samples were collected. Collected samples were stored at 4°C prior to use. Antibody-antigen interaction onto the porous surface of cryogel is illustrated in Fig. 5.

### 2.16. Protective antigen ELISA

Protective antigen concentrations remained in the solution at 15, 30, 45 and 60 min were determined using a competitive enzyme-linked immunosorbent assay (ELISA). Protective Antigen (PA) was diluted to a concentration of 0.5 μg/mL in the bicarbonate coating buffer and 100 μL were pipetted into each wells of a 96 well ELISA plate and incubated overnight, at 4 °C. Next day, the coating solution was aspirated. 300 μL of the blocking solution (PBS containing 1% casein), was pipetted into each well and incubated for 1 h, at room temp. The plate was washed 3 times with 350 μL of washing buffer (PBST) (PBS containing 0.05% Tween-20). Anti-PA antibody (PANG) was diluted at 1:3000 in the wash buffer. A series of PA standards at decreasing concentrations ranging from 1 to 0 μg/mL were prepared. Samples collected at different time points were diluted 1:2 in PBS. 50 μL of the standards or samples and 50 μL of the PANG antibody solution were pipetted into each well and incubated for 30 min at 37 °C. The plate was washed 3 × 350 μL with the washing buffer (PBST). 100 μL of anti-human antibody conjugated to horseradish peroxidase (anti-human-Ab-HRP) (Sigma, product no; A8667), diluted in the BioStab Antibody Stabilizer, at 1:50000, was pipetted into each well, and incubated for 30 min at 37°C. The plate was washed 3 × 350 μL with the washing buffer (PBST). 100 μL (3,3′,5,5′-tetramethylbenzidine substrate (TMB, Sigma) was pipetted into each well and incubated for 15 min at room temp in the dark. Reaction was stopped by pipetting 100 μL of 1 N HCl into each well. Optical densities (OD) at 450 nm were determined using an ELISA plate reader (ELX 800 microplate reader; BioTek Instruments, Inc., Winooski, VT). All standards and samples have been run in triplicates. The standard curve was created by plotting absorbance at 450 nm against PA concentration.

### 2.17. Statistical analysis

Data are presented as mean ± standard deviation for at least three replicates. Statistical analysis was performed using two-way ANOVA with the Bonferroni post-test, applying the correction for multiple comparisons at a significance level of $p < 0.05$ with Graph-Pad Prism 5 for Windows (GraphPad Software, USA).

## 3. Results

### 3.1. Material development and physical characterizations

A range of supermacroporous, continuous, monolithic, cryogel columns were synthesized by copolymerization of monomers in the frozen state, using monomer combinations of acrylamide (AAm) and allyl glycidyl ether (AGE) with N, N′ methylene-bis(acrylamide) (MBA) as a cross-linker, HEMA with MBA as a crosslinker, HEMA with PEGDA as a cross-linker in the presence of ammonium persulfate (APS)/N, N, N′, N′-tetra-methyl-ethylenediamine (TEMED) as an initiator/activator pair. A PVA-based cryogel was also synthesized using glutaraldehyde (1–2%) as a cross-linker. Fig. 2 shows schematically the steps required for the formation of a cryogel. Cryogels produced have large continuous interconnected pores (10–150 μm in diameter) that provide channels for the mobile phase to flow through. All cryogels were opaque, sponge like and elastic [Fig. 6A]. The gel phase (polymer with tightly bound water) comprised only 10% of the total cryogel volume, and the most of the monolithic column (90%) was an interconnected system of supermacropores filled with water [14,15]. The cryogel was easily compressed by hand to remove water accumulated inside the pores. When the compressed piece of cryogel was submerged in water, it acted as a sponge and within 1–2 s was restored to its original size and shape. All of the synthesized cryogels were able to maintain their shape without additional support [Fig. 6A]. The swelling degrees of equilibrium-swollen cryogels are shown in the Fig. 6B. The AAm-AGE cryogels had significantly higher swelling degree when compared to the other cryogels, while PVA, HEMA-MBA, and HEMA-PEGDA cryogels showed similar swelling degrees. The representative stress–strain curves for the various cryogel groups are displayed in Fig. 6C. All cryogels displayed a concave upward curve characteristic of elastomeric materials with large deformation. The elastic modulus (E) was calculated from the slope of the initial linear neo-Hookean region of the stress–strain (<20% strain) curves. Mechanical property data of all cryogels are

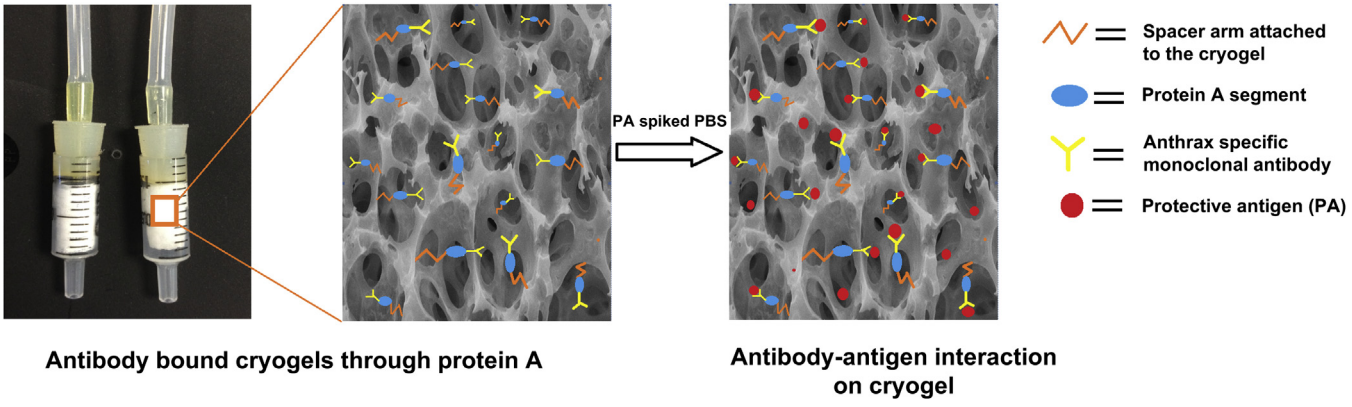


**Fig. 5.** Antibody bound adsorbent columns and cartoon illustrations showing antibody-antigen interactions within porous structure.

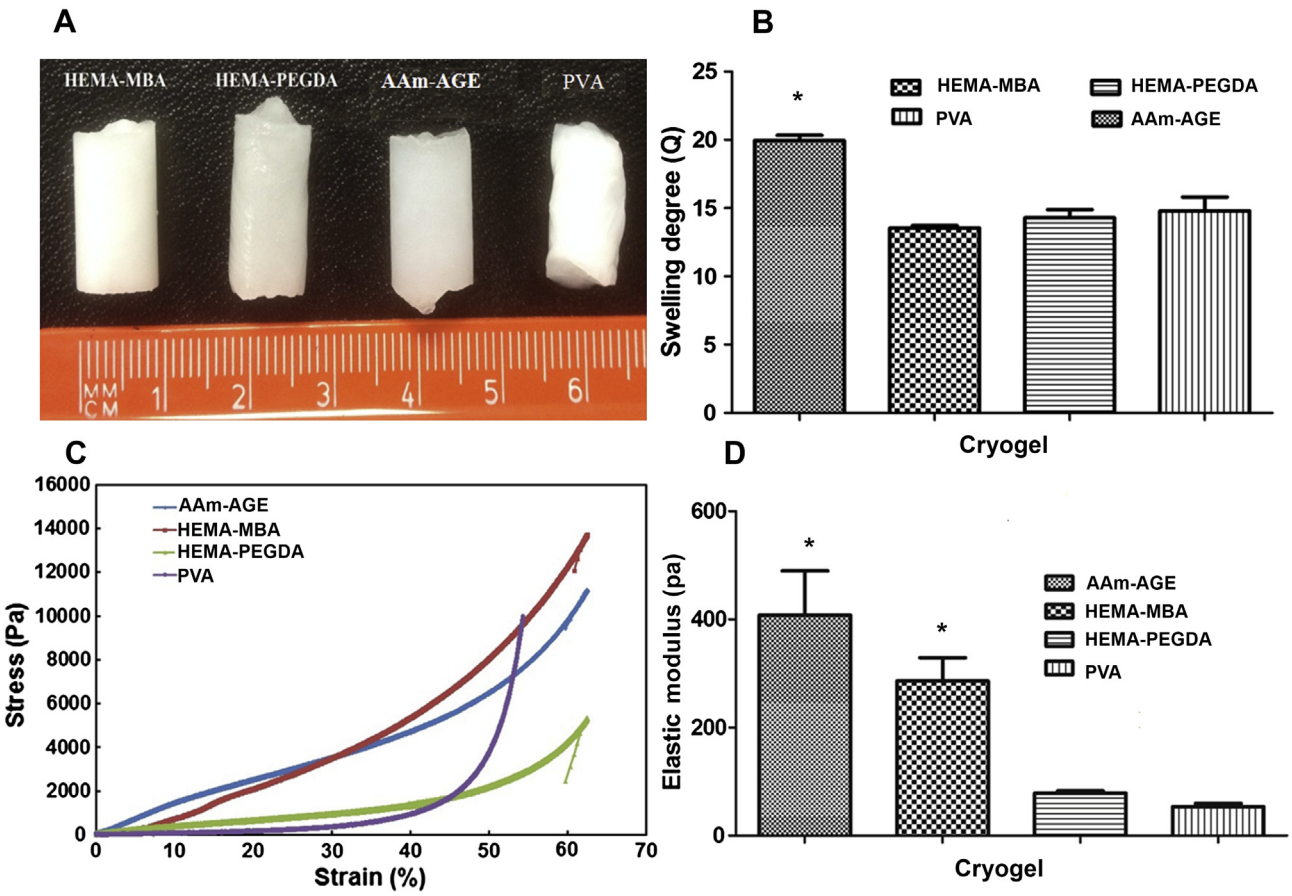


**Fig. 6.** Swelling and mechanical properties of cryogels; (A) macroscopic images, (B) swelling degrees, (C) representative stress–strain curves, and elastic moduli (D) of equilibrium-swollen cryogels. Values represent mean and standard deviation (n = 5). Data were compared using ANOVA with Bonferroni's post-hoc test (*$p < 0.05$).

summarized in Fig. 6D. AAm-AGE cryogels had significantly larger elastic modulus when compared to the other cryogels.

FTIR spectra (Fig 7d), show the bands which can be assigned to the N–H stretching vibration in the –NH group of N, N′- methylenebis(acrylamide) or the $-CONH_2$ groups of acrylamide in the hydrogels appear at 3470 and 1670 $cm^{-1}$. The C–H stretching band is characterized by the peak at 2960 $cm^{-1}$ due to symmetric or asymmetric stretching vibration of the $CH_2$ groups of acrylamide or N, N′-methylenebis(acrylamide). The peak near 1650 $cm^{-1}$ in Fig. 7d is the amide I band. Similarly, the peaks near 1540 $cm^{-1}$ (N–H bending vibration/C–N stretching vibration) and 1240 $cm^{-1}$ (C–N stretching vibration/N–H bending vibration) are called the amide II band, and amide III band, respectively. The peak near 3300 $cm^{-1}$ is thought to be N–H bending vibration and the peak near 1400 $cm^{-1}$ to result from protein side-chain COO-. The amide III band is usually weak in the FTIR spectroscopy but can be found in the region from 1250 to 1350 $cm^{-1}$. FTIR spectra of protein A immobilized cryogels have indicated the specific groups usually found in protein structures, such as amides I, II and III, at 1680-1620 $cm^{-1}$, 1580-1480 $cm^{-1}$ and 1246 $cm^{-1}$, respectively. FTIR spectrum in Fig. 7c is associated with PVA cross-linked by glutaraldehyde (PVA/GA). It can be observed that two important peaks at $\nu = 2860$ and 2730 $cm^{-1}$ of C–H stretching are related to aldehydes, a duplet absorption with peaks attributed to the alkyl chain. The C–O stretching at approximately 1100 $cm^{-1}$ in pure PVA is replaced by a broader absorption band (from $\nu = 1000$ to 1140 $cm^{-1}$), which can be attributed to the ether (C–O) and the acetal ring (C–O–C) bands formed by the crosslinking reaction of PVA with GA.

### 3.2. Porous morphology and surface area of the cryogel

All SEM micrographs presented in this section are representative of a number of micrographs taken of replicates of each material. The SEM micrograph of AAm-AGE cryogel illustrates the presence of channels with a diameter of approximately 50–100 μm formed in the voids of the dense thick polymeric walls (Fig. 8A). In addition, the channels do not have a uniform size or cylindrical shape. Instead, channels appear to narrow into smaller necks or widen into larger openings. Cross sections of the polymeric walls consisted of small pores having a diameter range of 2–10 μm. HEMA-PEGDA cryogels had vertical channels with a pore diameter range of 50–100 μm in width and 100–200 μm in length (Fig. 8B), while HEMA-MBA formed cryogels with thick walled interconnected pore channels with 20–100 μm pore diameter (Fig. 8C). PVA formed cryogels had irregular pore sizes and thin walled pores with a diameter of 10–150 μm (Fig. 8D). HEMA-PEGDA cryogels had very thin polymer walls with large, continuous interconnected pores that provide channels for the mobile phase to flow through. The pore size of the matrix is much larger than the size of the protein molecules, allowing them to pass through easily. The confocal microscopy images in Fig. 9A–D shows similar pictures to SEM images, but it shows the cryogels internal porous structure in hydrated conditions. It is clearly seen that even in hydrated state cryogels have large pores (dark voids) and thin polymer walls (with red fluorescence).

Nitrogen adsorption isotherms, calculated as the amount of $N_2$ adsorbed as function of the relative pressure at −196°C, are shown

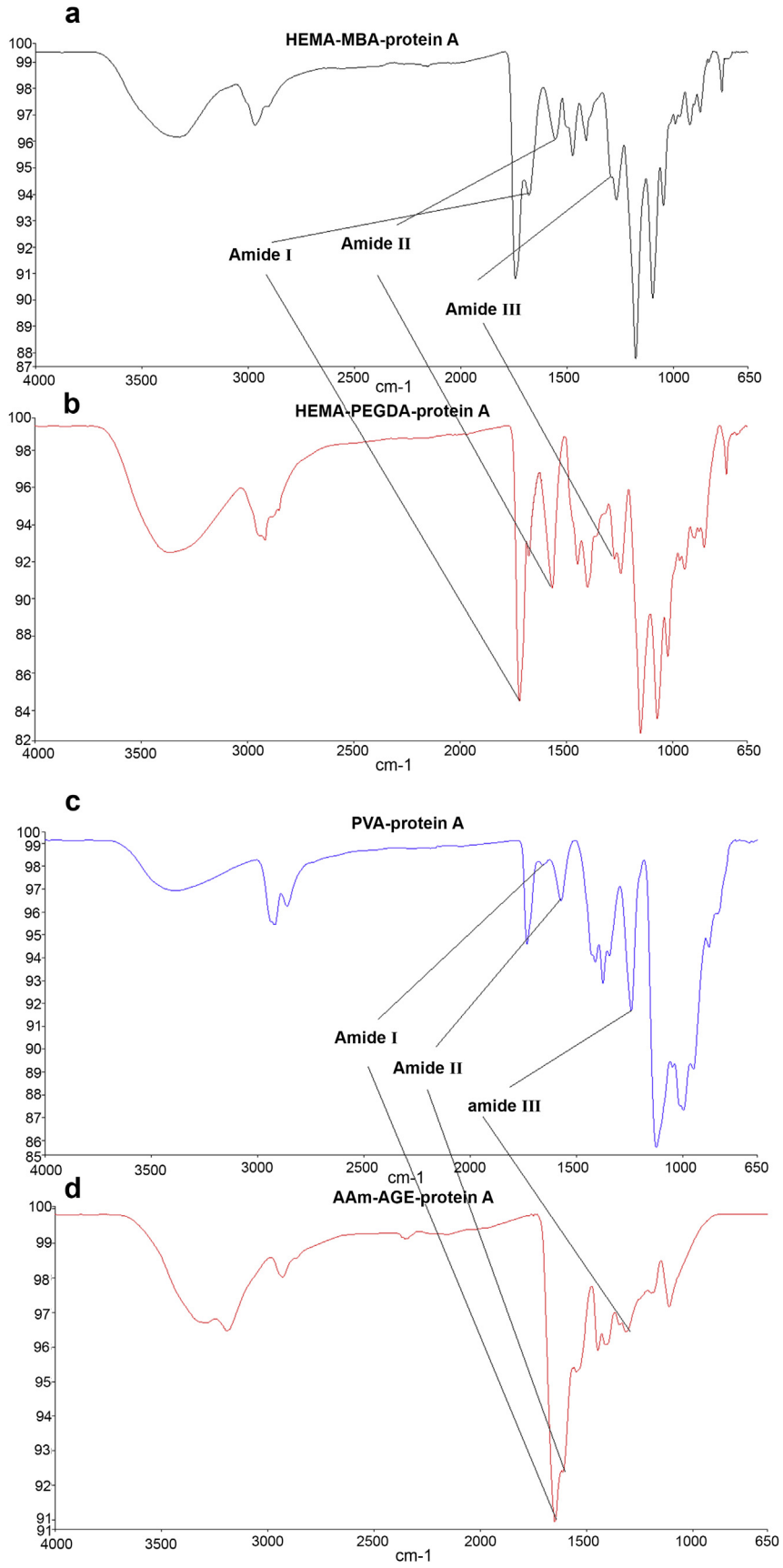


**Fig. 7.** FTIR spectrum of protein A attached a) HEMA-MBA; b) HEMA-PEGDA; c) PVA and d) AAm-AGE cryogels. Amides I, II and III peaks, at 1680–1620 $cm^{-1}$, 1580–1480 $cm^{-1}$ and 1246 $cm^{-1}$, respectively confirm the covalent attachment of protein A on the cryogel surface.

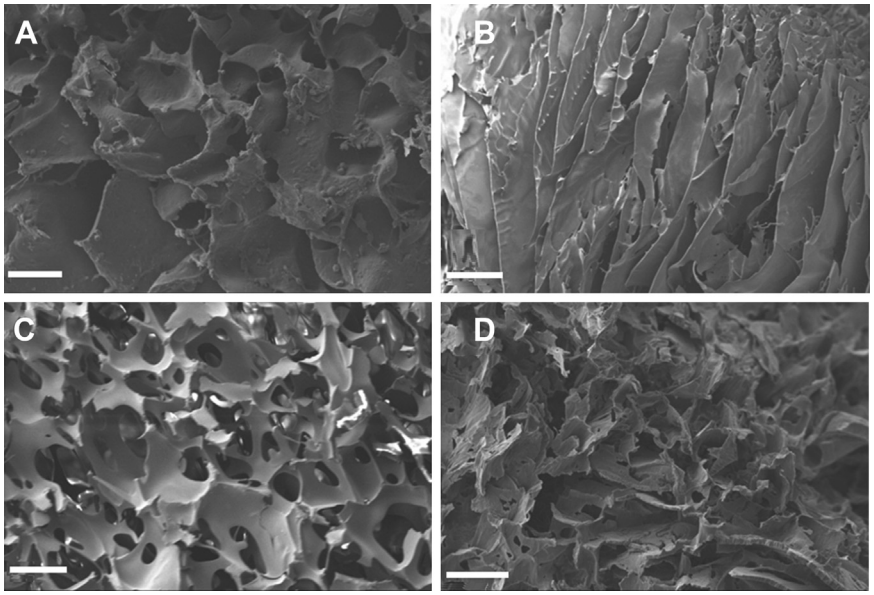


**Fig. 8.** Representative SEM images of (A) AAm-AGE, (B) HEMA-PEGDA, (C) HEMA-MBA, and (D) PVA cryogels illustrating porous internal structures. Scale bar = 100 μm.

in Fig. 10. Adsorption Isotherms of AAm-AGE (Fig. 10A), HEMA-MBA (Fig. 10B) and PVA (Fig. 10D) are of type IV with a hysteresis loop associated with mesoporous materials. Meso-porosity increased the specific surface area in the cryogel material when compared to the HEMA-PEGDA cryogel, making the specific surface area as high as 194.854 $m^2/g$ for HEMA-MBA and 101.319 $m^2/g$ for the AAm-MBA cryogel (Table 1). The decrease in specific surface area is mostly connected with the decrease in mesoporous surface area [Table 1].

### 3.3. Cryogel cytotoxicity and cell viability

The LDH assay results of sample extract cytotoxicity following 24 h of cell exposure to extract are displayed in Fig. 11. Following 24 h of 50% and 100% extract treatment, the positive controls incubated in dibutyltin maleate extract displayed cytotoxicity (73–75% cytotoxicity) ten times higher than that of the negative, culture medium control (6–7% cytotoxicity). The LDH assay revealed that, after 24 h of incubation, the 100% AAm-AGE extract

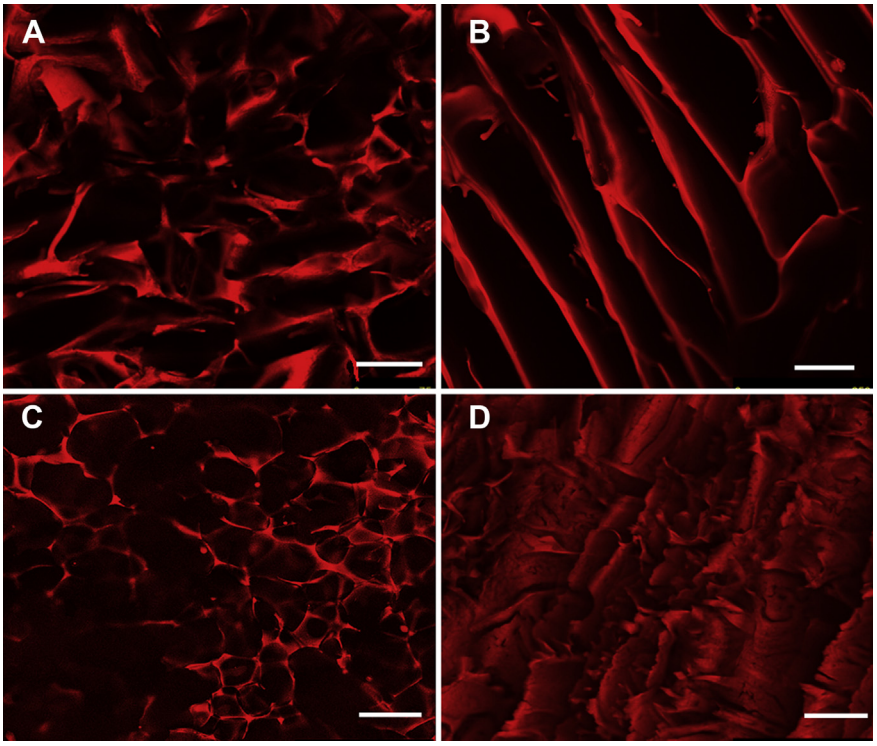


**Fig. 9.** Representative two dimensional (2D) confocal microscopy images of hydrated (A) AAm-AGE, (B) HEMA-PEGDA, (C) HEMA-MBA, and (D) PVA cryogels stained with Rhodamine B fluorescent dye. The red fluorescence dye stains the cryogel wall, and the dark areas are the channels within the matrix. Scale bar = 100 μm. (For interpretation of the references to colour in this figure legend, the reader is referred to the web version of this article.)

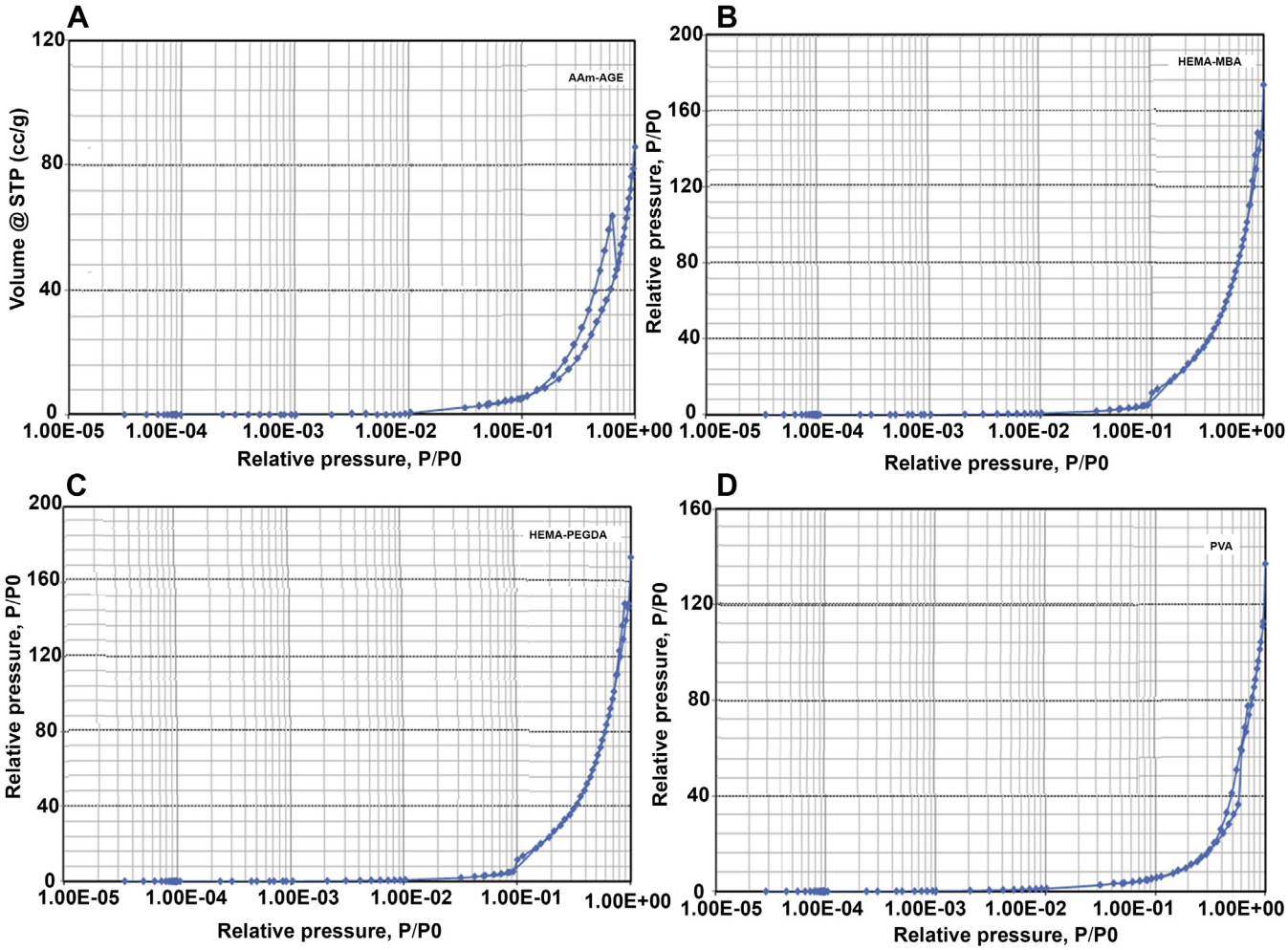


**Fig. 10.** Nitrogen adsorption–desorption isotherms, as the amount of $N_2$ adsorbed as a function of relative pressure for cryogel samples: (A) AAm-AGE, (B) HEMA-MBA, (C) HEMA-PEGDA, and (D) PVA.

induced up to 28% cytotoxicity towards V79 cells and the 50% PVA extract induced as little as 10% cytotoxicity. The MTS results in Fig. 12 show that the addition of extracts from the cryogel columns materials had no negative effect on cell metabolism after 24 h of cell incubation with 100% and 50% cryogel extract. In fact, the V79 cells maintained viability up to 121% after 24 h of incubation in the 50% HEMA-PEGDA extracts compared to the positive control after 24 h of treatment. The high viability of the cells might be an indication of cell proliferation or a signal that the cells are under stress. After 24 h contact with undiluted HEMA-MBA and AAm-AGE extracts, V79 cell viability was reduced to as low as 87% and 85%, respectively. However, when the cells were exposed to 50% dilution of HEMA-MBA and AAm-AGE extracts diluted in fresh culture medium, very little reduction in cell viability was observed compared to the negative control in which cells were treated with culture media alone. When the cells were treated with a 50% dilution of the extract in culture medium, an increase in cell survival was observed. The cells treated with both 50% and 100% PVA extracts for 24 h showed more than 99% of cell viability measured using the MTS assay. The LDH assay also indicated that both 50% and 100% extracts showed apparent cytotoxicity of less than 21% for V79 cells except AAm-AGE cryogels which showed minimal cytotoxicity (28% with 100% extracts and 25% with 50% extracts). The MTS and LDH assay results showed that the viability and membrane integrity of V79 cells after 24 h of 100% and 50% cryogel extract treatments were very close to the control treatments in which cells were exposed to the cell culture medium, indicating that the cryogel extracts did not cause cytotoxic effect during the 24 h exposure time.

### 3.4. Adsorption of PA from PBS by PANG and Valortim® bound AAm-AGE cryogel columns

Table 1 shows the adsorption capacity of protein-A and antibody onto the different cryogels. The binding study on cryogel samples

**Table 1**
Specific surface area and binding capacities of cryogel towards protein A, PANG antibody and Valortim® antibody.

| Cryogel | BET surface area ($m^2$/g) | Protein-A (mg/g of adsorbent)[a,b] | PANG (mg/g of adsorbent)[a,b] | Valortim® (mg/g of adsorbent)[a,b,c] |
|---|---|---|---|---|
| AAm-AGE | 101.319 | 96.4 ± 10.4 | 108.0 ± 19.3 | 117.0 ± 13.4 |
| HEMA-MBA | 194.854 | 47.3 ± 13.4 | 58.7 ± 11.2 | 72.3 ± 11.0 |
| HEMA-PEGDA | 69.837 | 38.3 ± 8.6 | 46.3 ± 9.3 | 49.8 ± 20.3 |
| PVA | 84.881 | 84.2 ± 15.5 | 92.3 ± 21.4 | 95.2 ± 7.4 |

All values are reported as mean ± standard deviation, n = 3.
[a] There were no statistically significant differences among HEMA-MBA, HEMA-PEGDA and PVA.
[b] Statistically significant differences between AAm-AGE and HEMA-PEGDA ($p < 0.05$).
[c] AAm-AGE-Valortim® was statistically significant from AAm-AGE-PANG ($p < 0.05$).

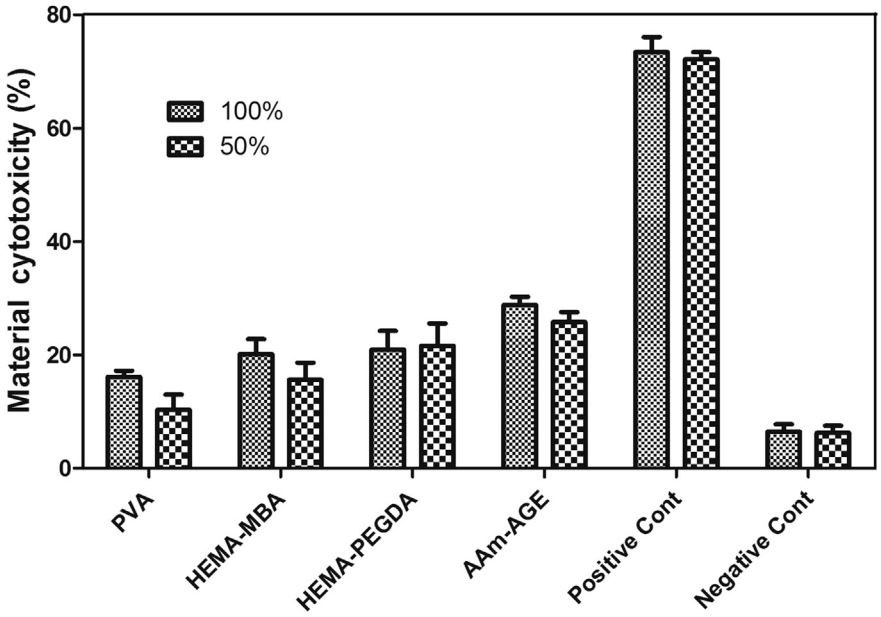


**Fig. 11.** The cytotoxicity of cryogel extracts determined by LDH assay.

revealed that the AAm-AGE cryogel column displayed a 2.5-fold increase in protein-A binding capacity relative to the HEMA-PEGDA cryogels (96.4 ± 10.4 mg/g vs 38.3 ± 8.6 mg/g). However, protein-A capacities among HEMA-MBA, HEMA-PEGDA and PVA were not statistically significant from each other (Table 1). PANG and Valortim® antibody binding capacity to the AAm-AGE-protein A cryogels increased by 2.3-fold relative to HEMA-PEGDA-PANG and 2.4-fold relative to the HEMA-PEGDA-Valortim® cryogel ($p < 0.05$). No significant differences were found in antibody binding capacity among the HEMA-MBA-PANG, HEMA-PEGDA-PANG and PVA-PANG or HEMA-MBA-Valortim, HEMA-PEGDA-Valortim and PVA-Valortim cryogel groups. The antibody binding capacity of the AAm-AGE-protein A cryogel column was significantly higher ($p < 0.05$) for Valortim® (117 mg/g) than for PANG (108 mg/g).

ELISA results showed that unmodified AAm-AGE cryogels as well as the AAm-AGE-protein A columns did not remove PA from solution over the 60 min recirculation sampled at 10, 30, 45 and 60 min time points (Fig. 13). In contrast, the AAm-AGE-Valortim cryogel columns removed 87% (1–0.13 μg/mL) of PA from solution over 60 min recirculation and the AAm-AGE-PANG cryogel column removed 59% PA over 60 min recirculation. The PA concentration remained in the AAm-AGE-protein-A-Valortim group decrease by 79% relative to control unmodified AAm-AGE group ($p < 0.05$), while it decreased 81% relative to control AAm-AGE-protein A group ($p < 0.05$), over 60 min. Similarly, the PA concentration remained in the AAm-AGE-protein-A-PANG group decreased by 47% relative to control unmodified AAm-AGE group ($p < 0.05$), while it decreased 52% relative to control AAm-AGE-protein A group ($p < 0.05$), over 60 min. These results strongly indicated that

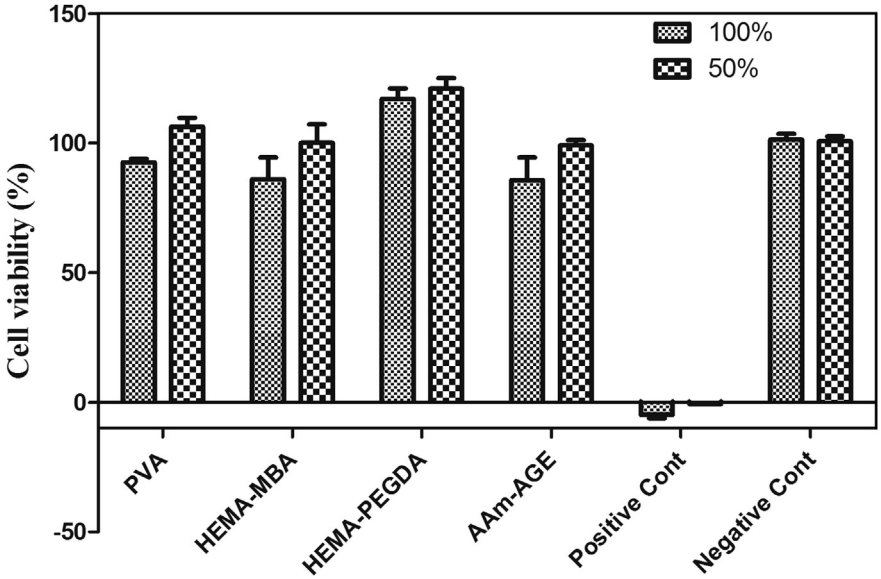


**Fig. 12.** V79 cell viability was determined by MTS assay after 24 h incubation with cryogel extracts. Cells were treated with DMEM and dibutyltin maleate containing PVC polymer for negative and positive controls, respectively.

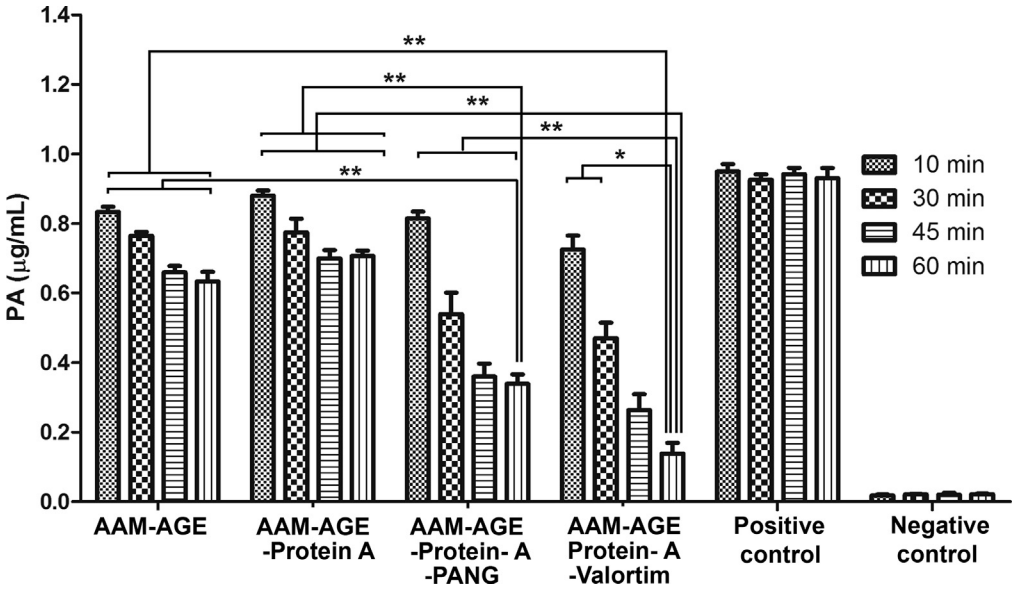


**Fig. 13.** The concentration of PA remained in the solution at each of the time points for the individual cryogel adsorbent type. Values represent mean and standard deviation (n = 3). Data were compared using two-way-ANOVA with Bonferroni's post-hoc test (*p < 0.05). *Values indicate significant differences from the other time points in same cryogel group (p < 0.05), while ** values indicate statistically significant differences in comparison with other cryogel groups (p < 0.05).

the PA adsorption from PBS by Valortim® bound cryogel column was considerably higher than the PANG bound cryogel column, over 60 min of recirculation.

## 4. Discussion

Increasing concern over bioterrorism and biological warfare involving *B. anthracis* in recent years has put the effort to discover and develop anti-anthrax agents on a high-priority list. Recently, a growing interest has been shown in using cryogels as adsorbents for diverse applications including bio-separations, bio-catalysis, chromatography, monolayer cell separation, protein purification, biomedical therapy [42–44] and regenerative medicine [45–47]. A high-affinity anthrax toxin specific monoclonal antibody therapeutic that targets anthrax toxins would be an important therapeutic addition to the options for prophylaxis and treatment of anthrax. Generating a material capable of specifically binding anthrax toxin while at the same time non-specifically binding inflammatory mediators such as cytokines, would be ideal for a passive barrier. The overall objective of the current study was to develop the supermacroporous biologically compatible synthetic cryogel adsorbent material with immobilized protein A for covalent attachment of anthrax toxin specific monoclonal antibodies and to evaluate the ability of these antibody bound cryogel materials to remove anthrax toxin protective antigen as an effective therapy for the treatment of *B. anthracis* infection. Such a therapy would be appropriate for use when post *B. anthracis* exposure beyond the therapeutic window for oral antibiotic efficacy.

A supermacroporous AAm-AGE, PVA, HEMA-MBA, and HEMA-PEGDA cryogels were produced by copolymerization in the frozen state in the presence of APS/TEMED. The hydroxyl and epoxy groups on the cryogel backbone allowed modification with protein A. The radical copolymerization of acrylamide (main co-monomer), N, N′-metylene-bis(acrylamide) (cross-linker) and allyl glycidyl ether (minor co-monomer used to introduce epoxy groups into the cryogel structure; the epoxy groups are used further for the covalent immobilization of affinity ligands (i.e. protein A and antibodies). The hydroxyl groups present on the PVA, HEMA-PEGDA, and HEMA-MBA cryogels were activated by cynogen bromide (CNBr) activation. Activation with CNBr yields reactive imidocarbamates that react with amine groups in proteins to form a peptide bond. In epoxy containing AAm-AGE cryogel, steric hindrance between immobilised ligand (protein) and large target molecules can occur during the interaction with immobilised protein. To overcome this problem the protein A was coupled to the epoxy-containing supermacroporous cryogel matrix through a spacer arm. The two-step derivatization includes reaction with ethylenediamine followed by the reaction with glutaraldehyde giving a spacer arm. This introduced aldehyde groups on the cryogel surface. Coupled aldehyde groups react mostly with primary groups on the protein to form reversible Schiff bases. These Schiff bases can be reduced to form stable covalent links using a reducing agent such as sodium borohydride. Protein A was coupled to the reactive derivatives of cryogels through its amine groups. The introduction of the spacer is assumed to improve the covalent cross-linking of IgG antibodies to the immobilised protein using dimethyl pimelimidate (DMP). DMP was used to permanently link antibody that has been bound by immobilized protein A. It binds free amino groups at pH range 7.0–10.0 to form amidine bonds.

On physical examination AAm-AGE, HEMA-MBA, and HEMA-PEGDA appeared stiff and mechanically stable, the liquid could flow through the gel matrix with very low resistance, indicating that these cryogels can be potential matrices for adsorbent columns. There were some differences in the swelling ratio which was found to be less in the HEMA-PEGDA and PVA-GA cryogels than in the AAm-AGE cryogel, indicating that AAm-AGE-MBA cryogels contain more water than other cryogels. All the cryogel materials have porous and thin polymer walls, large continuous interconnected pores (10–200 μm in diameter) that provide channels for the mobile phase to flow through. Moreover, the cryogel structures revealed by confocal microscopy align with the cryogel images obtained by scanning electron microscopy (SEM) which characterize the fine structures of porous materials but only in the dried state. The porous structures revealed by confocal microscopy and SEM at 10–100 μm scale were essentially the same. Confocal microscopy images of the Rhodamine B stained cryogels, confirmed a pore morphology which would allow biomolecules to flow through the internal channels of the cryogels. Such biomolecules as

protein A and antibodies with a size of 55 kD and 150 kD respectively could easily pass through pores of 10–100 μm diameter and could be covalently attached to the reactive functional surface groups available on the pore walls [48]. Nitrogen adsorption results showed that structural properties such as specific surface area and porosity depends on the type of monomer/cross-linker systems used in the synthesis. Bond formations between the polymer backbone and protein A molecules were confirmed by FTIR which showed that peaks at different wave numbers correspond to particular amide linkages and functional groups.

With the increasing protein content, a higher PANG and Valortim® binding may be expected. But this may not be advantageous in all cases due to possible geometric (i.e., steric) effects. Protein A molecule contains a tandem of five similar domains, each capable of binding the Fc region of antibodies. Each molecule of soluble protein is able to bind two molecules of PANG or Valortim® antibody. Steric hindrance prevents the binding of more than one or two PANG or Valortim® antibody molecules to the immobilized protein molecule. The large pore size in combination with highly interconnected pore morphology seen in the AAm-AGE cryogel provided a large surface area which resulted in a high protein binding capacity (96.4 ± 10.4 mg/g of adsorbent). In contrast, the large pore size in the HEMA-MBA and HEMA-PEGDA cryogel resulted in a small area available for ligand coupling and hence in a small protein A (38.3 ± 8.6 mg/g of adsorbent) binding capacity, which in turn resulted in low PANG (46.3 ± 9.3 mg/g adsorbent) and Valortim® (49.8 ± 20.3 mg/g of adsorbent) binding capacities. Smaller pores (>5 μm) within the walls of PVA cryogel also helps to increase the available surface area for ligand binding and hence PVA cryogel showed slightly higher protein A capacity and thus high antibody binding capacity relative to that of the HEMA based cryogels, as shown in Table 1.

Most glycosylation sites are found in the constant region of the heavy chain of an antibody [49,50] and glycosylation is believed to play an important role in antibody conformation, Fc receptor binding and half-life [51–55]. The significantly better binding of the glycosylated Valortim® antibody to the AAm-AGE-protein A cryogel column compared to the non-glycosylated PANG antibody would support this observation. This difference in cyryogel loading may explain in part the differences observed in PA recovery as the Valortim® bound cryogel column removed more PA from solution than the PANG bound cryogel column after 60 min. Others factors which may also have contributed to the differences in PA removal include inactivation of the binding capacity of the PANG antibody molecules upon coupling to protein A and poor antibody orientation post coupling. There is a possibility that de-glycosylation may have affected the binding affinity of PANG for PA.

The efficacy of these PANG and Valortim® bound cryogel biomaterials in adsorbing anthrax toxin PA *in vitro* suggest that this approach could be useful in developing therapeutically relevant agents to combat possible future risk of bioterrorism involving anthrax toxins.

## 5. Conclusions

In conclusion we have fabricated polymeric cryogel adsorbents having epoxy and hydroxyl functionalities with different cross-linkers by cryogelation technique. Matrices were found to be supermacroporous and having interconnected porous architecture with good swelling behaviour, mechanical strength and viscoelastic behaviour. We have explored for the first time the practical utility of these cryogel adsorbents with different physical and mechanical properties for binding of anthrax toxin specific antibodies, PANG and Valortim® through protein A affinity ligand. Further, we have also demonstrated for the first time that protein A bound cryogel AAm-AGE has properties most suited for use in binding of antibody for the removal of anthrax toxin PA and have highlighted differences in antibody properties which impact efficacy for this application. Further, the current study has conclusively demonstrated that the glycosylation status of the antibody has a positive effect on the efficiency of antibody binding to PA.

## Acknowledgements

This work was funded by the People Programme (Marie Curie Actions) of the European Union's Seventh Framework Programme, Industry-Academia Partnerships and Pathways (IAPP) project 'Adsorbent Carbons for the Removal of Biologically Active Toxins (ACROBAT-Grant agreement no. 286366 FP7-People-2011-IAPP)' and FP7-PEOPLE-RG project 'Novel smart materials for biomedical applications (BioSmart-Grant agreement no. PERG08-GA-2010-276954)'. The authors would like to thank PharmAthene Inc, (Annapolis, Maryland, USA) and Fraunhofer USA Inc, (Newark, Delaware, USA) for the kind gift of antibodies Valortim® and PANG, respectively.

## References

[1] Dixon TC, Meselson M, Guillemin J, Hanna PC. Anthrax. N Engl J Med 1999;341:815–26.
[2] Leppla SH. Anthrax toxins. In bacterial toxins and virulence factors in diseases. In: Moss J, Iglewski B, Vaughan M, Tu A, editors. Handbook of natural toxins. New York: Dekker; 1995. p. 543–72.
[3] Mohamed N, Clagett M, Li J, Jones S, Pincus S, D'Alia G, et al. A high-affinity monoclonal antibody to anthrax protective antigen passively protects rabbits before and after aerosolized Bacillus anthracis spore challenge. Infect Immun 2005;73:795–802.
[4] Hendricks KA, Wright ME, Shadomy SV, Bradley JS, Morrow MG, Pavia AT, et al. Centers for disease control and prevention expert panel meetings on prevention and treatment of anthrax in adults. Emerg Infect Dis 2014:20.
[5] Kummerfeldt CE. Raxibacumab: potential role in the treatment of inhalational anthrax. Infect Drug Resist 2014;7:101–9.
[6] Mett V, Chichester JA, Stewart ML, Musiychuk K, Bi H, Reifsnyder CJ, et al. A non-glycosylated, plant-produced human monoclonal antibody against anthrax protective antigen protects mice and non-human primates from B. anthracis spore challenge. Hum Vaccines 2011;7:183–90.
[7] Vitale L, Blanset D, Lowy I, O'Neill T, Goldstein J, Little SF, et al. Prophylaxis and therapy of inhalational anthrax by a novel monoclonal antibody to protective antigen that mimics vaccine-induced immunity. Infect Immun 2006;74:5840–7.
[8] Riddle V, Leese P, Blanset D, Adamcio M, Meldorf M, Lowy I. Phase I study evaluating the safety and pharmacokinetics of MDX-1303, a fully human monoclonal antibody against Bacillus anthracis protective antigen, in healthy volunteers. Clin Vaccine Immunol 2011;18:2136–42.
[9] Dainiak MB, Kumar A, Plieva FM, Galaev IY, Mattiasson B. Integrated isolation of antibody fragments from microbial cell culture fluids using supermacroporous cryogels. J Chromatogr A 2004;1045:93–8.
[10] Hanora A, Bernaudat F, Plieva FM, Dainiak MB, Bulow L, Galaev IY, et al. Screening of peptide affinity tags using immobilised metal affinity chromatography in 96-well plate format. J Chromatogr A 2005;1087:38–44.
[11] Le Noir M, Plieva F, Hey T, Guieysse B, Mattiasson B. Macroporous molecularly imprinted polymer/cryogel composite systems for the removal of endocrine disrupting trace contaminants. J Chromatogr A 2007;1154:158–64.
[12] Bolgen N, Plieva F, Galaev IY, Mattiasson B, Piskin E. Cryogelation for preparation of novel biodegradable tissue-engineering scaffolds. J Biomat Sci-Polym E 2007;18:1165–79.
[13] Dainiak MB, Allan IU, Savina IN, Cornelio L, James ES, James SL, et al. Gelatin-fibrinogen cryogel dermal matrices for wound repair: preparation, optimisation and in vitro study. Biomaterials 2010;31:67–76.
[14] Gun'ko VM, Savina IN, Mikhalovsky SV. Cryogels: morphological, structural and adsorption characterisation. Adv Colloid Interface Sci 2013;187–188:1–46.
[15] Savina IN, Gun'ko VM, Turov VV, Dainiak M, Phillips GJ, Galaev IY, et al. Porous structure and water state in cross-linked polymer and protein cryo-hydrogels. Soft Matter 2011;7:4276–83.
[16] Weber V, Linsberger I, Hauner M, Leistner A, Leistner A, Falkenhagen D. Neutral styrene divinylbenzene copolymers for adsorption of toxins in liver failure. Biomacromolecules 2008;9:1322–8.
[17] Pan ZF, Zou HF, Mo WM, Huang XD, Wu RN. Protein A immobilized monolithic capillary column for affinity chromatography. Anal Chim Acta 2002;466:141–50.
[18] Ehrhart JC, Bennetau B, Renaud L, Madrange JP, Thomas L, Morisot J, et al. A new immunosensor for breast cancer cell detection using antibody-coated

long alkylsilane self-assembled monolayers in a parallel plate flow chamber. Biosens Bioelectron 2008;24:467–74.
[19] Nagare GD, Mukherji S. Characterization of silanization and antibody immobilization on spin-on glass (SOG) surface. Appl Surf Sci 2009;255:3696–700.
[20] Blagoi G, Keller S, Johansson A, Boisen A, Dufva M. Functionalization of SU-8 photoresist surfaces with IgG proteins. Appl Surf Sci 2008;255:2896–902.
[21] Tedeschi L, Domenici C, Ahluwalia A, Baldini F, Mencaglia A. Antibody immobilisation on fibre optic TIRF sensors. Biosens Bioelectron 2003;19:85–93.
[22] Wang H, Liu YL, Yang YH, Deng T, Shen GL, Yu RQ. A protein A-based orientation-controlled immobilization strategy for antibodies using nanometer-sized gold particles and plasma-polymerized film. Anal Biochem 2004;324:219–26.
[23] Sapsford KE, Ligler FS. Real-time analysis of protein adsorption to a variety of thin films. Biosens Bioelectron 2004;19:1045–55.
[24] Oura K, Lifshits VG, Saranin AA, Zotov AV, Katayama M. Surface science—an introduction. Berlin: Springer; 2004.
[25] Koyama K, Yamaguchi N, Miyasaka T. Antibody-mediated bacteriorhodopsin orientation for molecular device architectures. Science 1994;265:762–5.
[26] Bright FV, Betts TA, Litwiler KS. Regenerable fiber-optic-based immunosensor. Anal Chem 1990;62:1065–9.
[27] Gebbert A, Alvarezicaza M, Stocklein W, Schmid RD. Real-time monitoring of immunochemical interactions with a tantalum capacitance flow-through cell. Anal Chem 1992;64:997–1003.
[28] Angenendt P, Glokler J, Murphy D, Lehrach H, Cahill DJ. Toward optimized antibody microarrays: a comparison of current microarray support materials. Anal Biochem 2002;309:253–60.
[29] Pavlickova P, Knappik A, Kambhampati D, Ortigao F, Hug H. Microarray of recombinant antibodies using a streptavidin sensor surface self-assembled onto a gold layer. Biotechniques 2003;34:124–30.
[30] Hermanson GT. In: Greg T, Hermanson A, Krishna M, Smith PK, editors. Immobilized affinity ligand techniques. San Diego, CA: Academic Press; 1992.
[31] Spitznagel TM, Clark DS. Surface-density and orientation effects on immobilized antibodies and antibody fragments. Nat Biotechnol 1993;11:825–9.
[32] Rao SV, Anderson KW, Bachas LG. Oriented immobilization of proteins. Mikrochim Acta 1998;128:127–43.
[33] Gersten DM, Marchalonis JJ. A rapid, novel method for the solid-phase derivatization of IgG antibodies for immune-affinity chromatography. J Immunol Methods 1978;24:305–9.
[34] Turkova J. Oriented immobilization of biologically active proteins as a tool for revealing protein interactions and function. J Chromatogr B Biomed Sci Appl 1999;722:11–31.
[35] Lu B, Smyth MR, O'Kennedy R. Oriented immobilization of antibodies and its applications in immunoassays and immunosensors. Analyst 1996;121:29R–32R.
[36] Babacan S, Pivarnik P, Letcher S, Rand AG. Evaluation of antibody immobilization methods for piezoelectric biosensor application. Biosens Bioelectron 2000;15:615–21.
[37] Anderson GP, Jacoby MA, Ligler FS, King KD. Effectiveness of protein A for antibody immobilization for a fiber optic biosensor. Biosens Bioelectron 1997;12:329–36.
[38] Danczyk R, Krieder B, North A, Webster T, HogenEsch H, Rundell A. Comparison of antibody functionality using different immobilization methods. Biotechnol Bioeng 2003;84:215–23.
[39] Stokes MGM, Titball RW, Neeson BN, Galen JE, Walker NJ, Stagg AJ, et al. Oral administration of a Salmonella enterica-based vaccine expressing Bacillus anthracis protective antigen confers protection against aerosolized B-anthracis. Infect Immun 2007;75:1827–34.
[40] Plieva FM, Karlsson M, Aguilar MR, Gomez D, Mikhalovsky S, Galaev IY, et al. Pore structure of macroporous monolithic cryogels prepared from poly(vinyl alcohol). J Appl Polym Sci 2006;100:1057–66.
[41] ISO Standardization. Biological evaluation of medical devices – part 5: tests for in vitro cytotoxicity. 2009.
[42] Bereli N, Andac M, Baydemir G, Say R, Galaev IY, Denizli A. Protein recognition via ion-coordinated molecularly imprinted supermacroporous cryogels. J Chromatogr A 2008;1190:18–26.
[43] Baydemir G, Bereli N, Andac M, Say R, Galaev IY, Denizli A. Bilirubin recognition via molecularly imprinted supermacroporous cryogels. Colloid Surf B 2009;68:33–8.
[44] Sun HX, Ge BS, Liu SN, Chen HL. Preparation of nitrocellulose (NC) immunoaffinity membrane for purification of rAPC antibody. J Sep Sci 2008;31:1201–6.
[45] Plieva FM, Galaev IY, Mattiasson B. Macroporous gels prepared at subzero temperatures as novel materials for chromatography of particulate-containing fluids and cell culture applications. J Sep Sci 2007;30:1657–71.
[46] Kumar A, Rodriguez-Caballero A, Plieva FM, Galaev IY, Nandakumar KS, Kamihira M, et al. Affinity binding of cells to cryogel adsorbents with immobilized specific ligands: effect of ligand coupling and matrix architecture. J Mol Recognit 2005;18:84–93.
[47] Hwang YS, Sangaj N, Varghese S. Interconnected macroporous poly(ethylene glycol) cryogels as a cell scaffold for cartilage tissue engineering. Tissue Eng Pt A 2010;16:3033–41.
[48] Noppe W, Plieva FM, Galaev IY, Vanhoorelbeke K, Mattiasson B, Deckmyn H. Immobilised peptide displaying phages as affinity ligands purification of lactoferrin from defatted milk. J Chromatogr A 2006;1101:79–85.
[49] Rothman RJ, Perussia B, Herlyn D, Warren L. Antibody-dependent cytotoxicity mediated by natural killer cells is enhanced by castanospermine-induced alterations of IgG glycosylation. Mol Immunol 1989;26:1113–23.
[50] Wright JF, Shulman MJ, Isenman DE, Painter RH. C1 binding by mouse IgM : the effect of abnormal glycosylation at position 402 resulting from a serine to asparagine exchange at residue 406 of the mu-chain. J Biol Chem 1990;265:10506–13.
[51] Huber R, Deisenhofer J, Colman PM, Matsushima M, Palm W. Crystallographic structure studies of an IgG molecule and an Fc fragment. Nature 1976;264:415–20.
[52] Winkelhake JL, Nicolson GL. Aglycosylantibody. Effects of exoglycosidase treatments on autochthonous antibody survival time in circulation. J Biol Chem 1976;251:1074–80.
[53] Koide N, Nose M, Muramatsu T. Recognition of IgG by Fc receptor and complement: effects of glycosidase digestion. Biochem Bioph Res Co 1977;75:838–44.
[54] Middaugh CR, Litman GW. Atypical glycosylation of an IgG monoclonal cryoimmunoglobulin. J Biol Chem 1987;262:3671–3.
[55] Tao MH, Morrison SL. Studies of aglycosylated chimeric mouse-human IgG. Role of carbohydrate in the structure and effector functions mediated by the human-IgG constant region. J Immunol 1989;143:2595–601.